REVIEW

A mini review on factors affecting network in thermally enhanced polymer composites: filler content, shape, size, and tailoring methods

Xiaoxiang He[1] · Dan Ou[1] · Shuying Wu[1] · Yue Luo[1] · Ying Ma[1] · Jingyao Sun[2,3]

Abstract

To enhance the thermal conductivity of polymers, a polymer composite system is an effective method, where types of thermally conductive fillers are often introduced into the polymer matrices to form special paths for the phonons or electrons. After years of studies, it can be concluded that selective fillers of different aspect ratio, size, and content and tailoring methods of filler network often result in multiple arrangements of filler network in space, which greatly affect the thermal conductivity of polymer composites. Thus, in this review, we summarize the main affecting factors of filler network, including the types, sizes, and shapes of fillers. Later, we discuss the latest progress of approaches to tailor the filler networks and outline the challenges and prospects of thermally conductive polymer composites.

Keywords Fillers · Tailoring methods · Filler network · Thermal conductivity · Polymer composites

1 Introduction

Polymers have advantages of lightweight, low cost, corrosion resistance, and easy processing, so they have received great attention in electronics, engineering, energy, and aerospace fields for heat dissipation [1–5]. Since most polymers are thermal insulators, to date, special attention has been focused on the thermally conductive polymer composites (TCPCs), where thermally conductive fillers are often introduced to form special paths to transport thermal energy [6–9]. For the samples requiring both thermal conductivity (TC) and electrical conductivity, metallic fillers (e.g., copper nanowires (CuNWs), silver nanoparticles (AgNPs)) and carbon-based fillers (e.g., graphite, carbon fibers (CFs), carbon nanotubes (CNTs), graphene) are often utilized; for the samples, only requiring TC, ceramic fillers (e.g., aluminum oxide (Al_2O_3), aluminum nitride (AlN), boron nitride (BN), silicon nitride (Si_3N_4), and silicon carbide (SiC)) are often used.

Over the past few decades, researchers have come up with various approaches to enhance the TC of TCPCs, for instance, to enhance the intrinsic TC of polymer, modify polymer/filler interfaces, search novel fillers with high intrinsic TC, and design and construct spatially continuous filler networks in TCPCs [10–14]. Herein, studies have indicated that forming continuous networks is one of the most effective and promising methods to achieve a high TC for TCPCs [15–17]. It has been concluded that filler content, filler aspect ratio, and filler size greatly affect the network. Generally, high filler content has already been widely reported to successfully form the networks, but it always deteriorates the mechanical and processing properties of TCPCs. A non-monotonous change in the TCs induced as the filler content increase also has been reported, since the failed network was always caused by the agglomeration of fillers. Fiber-like or platelet-like fillers are

✉ Ying Ma
cdmmy@foxmail.com

✉ Jingyao Sun
sunjingyao@mail.buct.edu.cn

Xiaoxiang He
heshosha@163.com

Dan Ou
2496905286@qq.com

Shuying Wu
wusy2015@xtu.edu.cn

Yue Luo
luoyue@xtu.edu.cn

1   School of Mechanical Engineering, Xiangtan University, Xiangtan 411105, China

2   College of Mechanical and Electrical Engineering, Beijing University of Chemical Technology, Beijing 100029, China

3   State Key Laboratory of Molecular Engineering of Polymers, Fudan University, Shanghai 200433, China

preferred than spherical fillers to build the networks due to their high aspect ratio, while they often trigger anisotropic TCs of TCPCs, which may not be needed in some TCPCs requiring isotropic TCs. Spherical fillers offer a high level of viscosity percolation threshold because they point contact in polymer matrices. This is benefit for the filler networks and the processing ability of TCPCs. So, nowadays, novel methods, such as spray-drying and spray-freeze-drying, have been developed to prepare the spherical fillers from other two shapes. Fillers can present different effects on the filler network since they often have a size from nanometers to millimeters. So, factors of filler-specific surface area, filler surface energy, filler–polymer interfacial thermal resistance, filler/filler contact areas, etc., have already been comprehensively studied in the literature. In addition, the filler networks greatly depend on the constructing methods without more filler content. Up to date, methods of 3D self-assembled network, double continuous network, segregated filler network, hybrid fillers, filler orientation, and other novel methods, such as forming method and ice-templated method, have already been proposed. In this review, we firstly focused on the affecting factors of filler network. After that, a critical review of the latest developments in the approaches to tailor filler networks is presented. Finally, the challenges and prospects of TCPCs are discussed. We hope that this review is helpful for the researchers to make TCPCs with high TC, yet light weight.

2 Influencing factors of the filler network

Both the theoretical and experimental results indicate that the formation of the continuous filler network is significant as it can greatly allow phonons or electrons to transport within the TCPCs. The filler content, filler aspect ratio, and filler size are the main parameters that largely influence the building of filler network. Thus, it is necessary for us to take a comprehensive view on these factors.

2.1 Filler content

Generally, theoretical and most experimental results have shown that a monotonous increase in TCs (Fig. 1a) was expected because the stable networks were gradually formed as fillers were employed with a increasing content [18–22]. Fillers are difficult to form a continuous path or network as the filler content is low, so a large loading level (often higher than 30 vol%) is always introduced into the polymer matrix [3], but the percolation threshold similar to electrical conductivity was seldom reported in TC as filler content increasing, except for only some fillers with extremely high TC, such as graphdiyne [23] and grapheme [24–26]. Also, it should be noted that the excessively high filler content is not always desired because it always deteriorates the mechanical and processing properties of TCPCs [27, 28]. For example, Kim et al. [29] reported a TC value of 2.92 W/(mK) after incorporating 70 wt% of BN into the ETDS matrix. For this extent of TC enhancement, very high filler loadings are required. This can result in increased density of ETDS composites, loss in mechanical properties, processing difficulties, and increased cost. Meanwhile, the content of fillers has a limitation; for example, the theoretical maximum addition volume fraction is 0.637 [30] as the spherical fillers dispersed randomly in polymer matrix.

Some experimental results have reported a non-monotonous change in the TCs as increasing the filler content, especially in the TCPCs with the nanoscale fillers (Fig. 1b), which attributes to the failed network caused by the agglomeration of fillers [31, 32]. Patti and co-workers [31] studied the TC of polypropylene/MWCNT composites. It was concluded that TCs changed in a non-linear trend via varying the amount of MWCNTs because the dispersion of MWCNTs often leads to uneven filler distribution, characterized by dispersed and agglomerated areas. Similar results also happened in the modified BN/polyvinylidene fluoride composites [33] and BN/poly(lactic-co-glycolic acid) composites [34].

Fig. 1 (**a**) A monotonous increasing [18] and (**b**) non-monotonous change [31] in TC as increasing the filler content (Images reprinted with permission from [16] and [27].)
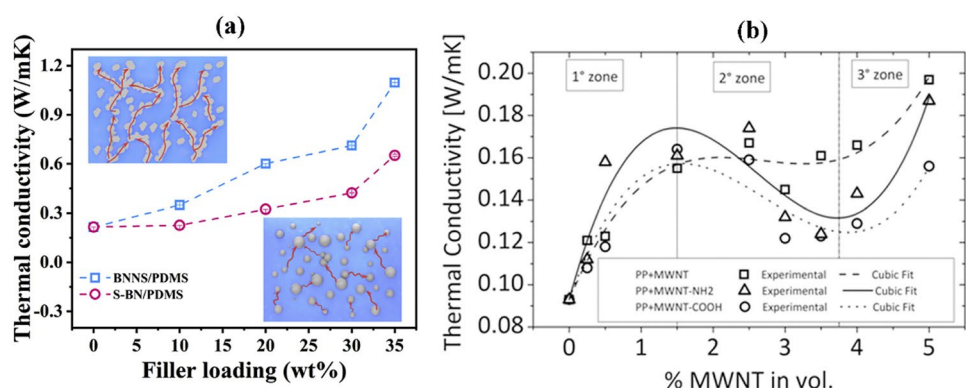
2.2 Filler shape

Fillers can be catalogued as fiber-like fillers or quasi-1D fillers (e.g., CF, CNT, and CuNW), platelet-like fillers or quasi-2D fillers (e.g., graphene, graphite, BN, and AlN) and spherical fillers (e.g., AlN, Al_2O_3) based on the aspect ratio.

Generally, fiber-like and platelet-like fillers are preferred to build the filler networks due to their high aspect ratio [35–39]. For example, Kim et al. [40] studied the effect of AlN shape on the TCs of TCPCs. It was found that AlN platelets triggered a TC almost 1.5 times higher than AlN spheres in the polyvinyl alcohol matrix with the same filler content of 50 vol%. Fiber-like or platelet-like fillers afford anisotropic TC, characterized by a much higher TC along the longitudinal (fiber-like fillers) or the in-plane direction (platelet-like fillers) than that along the perpendicular direction. So far, these fillers, such as BN [41–43] and grapheme [44–46], have already been widely used to prepare anisotropic TCPCs. The methods to prepare these TCPCs were discussed in the following part.

Spherical fillers often offer a fairly high level of viscosity percolation threshold because these fillers are point contact in polymer matrices, which is benefit for the filler networks and the processing ability of TCPCs [47]. Some researchers even developed methods (e.g., spray-drying [48, 49], spray-freeze-drying [50]) to prepare the spherical fillers from other fillers with intrinsic high TC. Su et al. [51] used the spray-drying technique to prepare the spherical BN particles from plate-like h-BN particles. The TC of spherical BN/PU composite was improved to 7.302 W/mK due to the well continuous networks, higher than that of platelet-like BN/PDMS composite with the same filler content of 40 wt%. Ren et al. [52] came up with a spray-assisted self-assembly approach to fabricate spherical BNs from plate-like BNs. The TC of spherical BN/PDMS composite was improved to 2.30 W/mK, almost fourfold higher than that of platelet-like BN/PDMS composite with the same filler content of 50 wt%, but with a much lower viscosity.

2.3 Filler size

Generally, thermally conductive fillers have a size from nanometers to millimeters, which presents different effects on the TCs of TCPCs. On the one hand, it has been reported that the TCs of TCPCs decrease as the filler size decreases. For example, Shin et al. [53] investigated the TCs of the BN/HDPE composite with different BN sizes. It was concluded that the TCs of the BN/HDPE composite decreased by 1.18 times from 4.5 W/(mK) to 3.8 W/(mK) as BN size decreases from 20 to 3 μm at filler content of 50 vol%. Similar results have also been reported in PVDF-HFP composites with graphene flake [54] and

epoxy composites with BN [55]. This phenomenon can be explained by the following reasons. Firstly, fillers with smaller size often have larger specific surface areas, and this easily creates more filler–polymer interfacial thermal resistance, i.e., it easily causes phonon scattering and hinders phonon transporting; secondly, fillers with a larger size easily create more stable paths or networks because of the formed larger contact area [56]. In addition, agglomeration often occurs as the filler size decreases due to the differences of surface energies and surface chemistries between fillers and polymer matrices, which significantly restrict the formation of filler network [57, 58].

On the other hand, some contradictory results have also been reported, i.e., smaller particles were easier to trigger a higher TC. For example, Zhou et al. [59] investigated the TCs of BN/HDPE composites as particle sizes decreasing from 15 to 0.5 μm. It was concluded that the TCs of BN/HDPE composite increased by 1.12 times from 1.05 W/(mK) to 1.18 W/(mK). This phenomenon was explained that since the absorption energy between smaller size fillers and HDPE particles was much higher compared with the larger size fillers, more stable filler paths were easily formed by the former. Zhang et al. [60] described relatively similar results in HDPE/Al_2O_3 composites, where Al_2O_3 with 4 different sizes from 0.1 to 10.0 μm were mixed with HDPE. The results indicated that the HDPE composites with smaller size fillers had the larger TC than larger ones at the same filler content because the smaller size particles can form filler pathways or networks more easily due to the large specific surface area and high surface energy.

In summary, it is important to consider the mechanical and processing properties of TCPCs simultaneously, when high content fillers are used to construct the networks. Although the fillers with high aspect ratio are efficient to build the networks, the anisotropic TCs are always obtained, which may not be needed in some polymer composites requiring isotropic TCs. Spherical fillers are also significant to the network since they offer a high level of viscosity percolation threshold. Nowadays, this triggers the tendency to explore spherical fillers from other shapes. Due to the size of fillers ranging from nanometers to millimeters, fillers present different effects on the filler network, so it is necessary for us to comprehensively consider the affecting factors of specific surface area, surface energy, filler–polymer interfacial thermal resistance, filler-filler contact area, etc.

2.4 Filler network tailoring method

The filler network also greatly depends on the preparing methods. Nowadays, scholars have proposed several types of methods to control the formation of filler network. Many methods to tailor filler network have been summarized here.

2.4.1 3D self-assembly network

The self-assembly network usually takes place as increasing the filler content above the percolation threshold, where the possible aggregation forces of the fillers, including van der Waals force, electrostatic force, liquid bridge, and hydrogen bonding, are larger enough than the resistant forces of steric repulsion and electrostatic repulsion; thereby, the fillers agglomerate with the adjacent fillers to form a self-assembled network [61, 62]. According to this theory, for electrically conductive polymer composites, a filler content above the percolation threshold was always reported to trigger 2–3 orders of enhancement in electrical conductivity [63], but for TCPCs, a much higher filler content (often larger than 30 vol%) was required to allow the fillers to directly contact to transport phonons [64, 65]. Embedding a high filler content, however, always leads to poor processing ability, poor mechanical properties and high cost. Thus, artificially controlled 3D self-assembled filler networks have been created without further filler content, such as forming method and ice-templated method.
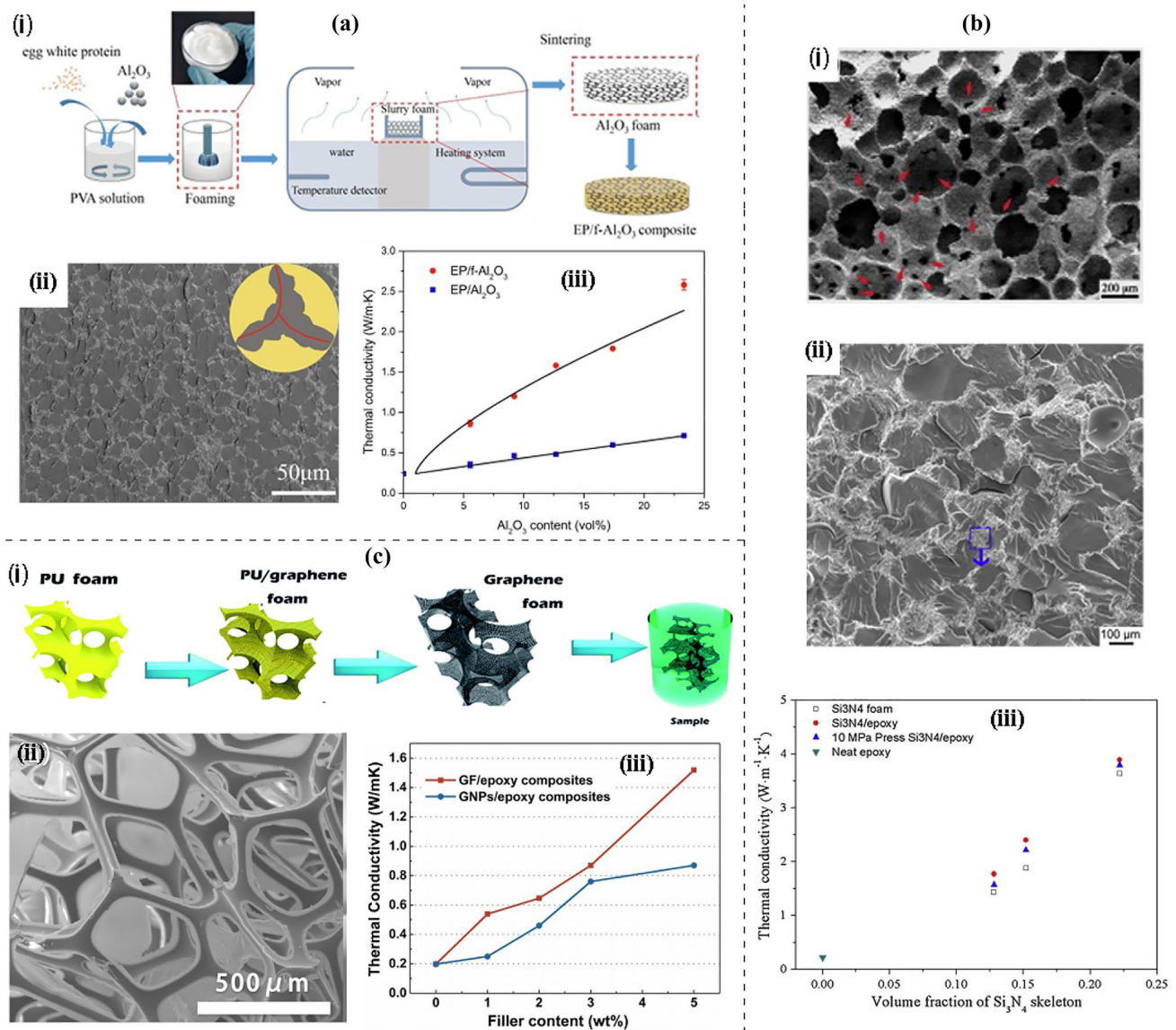

Fig. 2 (**a**) (i) Diagram of the preparation of filler network via egg white protein; (ii) SEM image of continuous filler network; and (iii) TCs of TCPCs as a function of filler content [66]. (**b**) (i) and (ii) SEM images of continuous filler network and polymer composite; (iii) TCs of TCPCs as a function of filler content [67]. (**c**) (i) (a) Diagram of the preparation of the filler network via commercial PU sponge; (ii) SEM image of continuous PU framework; (iii) TCs of TCPCs as a function of filler content[68]. (Images reprinted with permission from [61–63].)

Fig. 3 (**a**) Schematic illustration of the preparation of TCPCs by the cotton candy-templating method. (**b**) SEM image of TCPCs with continuous pathway. (**c**) TCs of the TCPCs as a function of filler content [65]. (Images reprinted with permission from [65].)
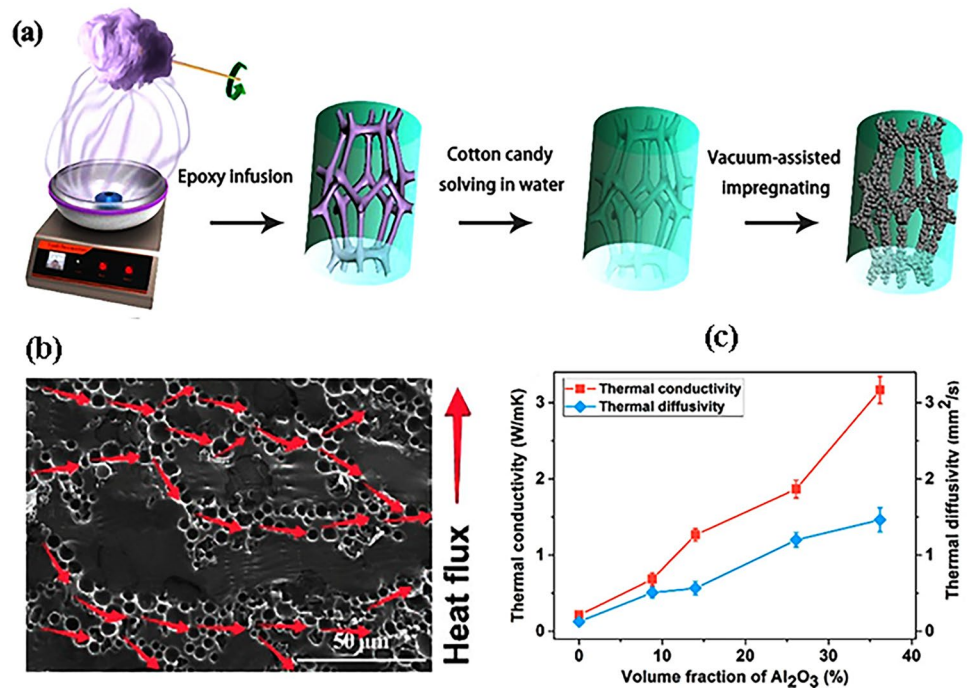
Foaming method Foaming method is a promising route to construct filler network without so much filler content. This method is always combined with infiltration to prepare polymer composites. Up to date, 3D protein forming, commercial sponge, and cotton candy-templating have already been developed to prepare the foam structure. For example, Xiao et al. [66] used the egg white protein to fabricate a honeycomb-like Al_2O_3 network (Fig. 2a(i and ii)). The TC of epoxy composite reached to 2.56 W/(mK) at 23.32 vol%, 3.6-fold higher than epoxy composite with random dispersion of Al_2O_3 (Fig. 2(a–iii)). Yin et al. [67] used the protein forming method to prepare the continuous sintered Si3N4 network (Fig. 2b(i)). The epoxy solution was then infiltrated into the Si3N4 foams by using a vacuum-assisted resin impregnation method (Fig. 2b(ii)). The TC of epoxy composite reached 3.89 W/(mK) at 22.2 vol%, 17-fold higher than neat epoxy (Fig. 2b(iii)). Liu et al. [68] obtained a 3D graphene foam (GF) based on the commercial PU sponge, followed by infusing the homogeneous epoxy solution cured at temperature of 165 °C for 14 h (Fig. 2c(i and ii)). The GF/polymer composites exhibited a TC up to 1.52 W/(mK) at a filler content of 5.0 wt% (Fig. 2c(iii)). Later on, Liu et al. [69] further developed the GF via sacrificial commercial polyurethane sponge template. The epoxy composite with a TC of 8.04 W/(mK) at a filler content of 6.8 wt% was obtained.

Inspired by the cotton candy, Wu et al. [70] constructed a facile and eco-friendly Al_2O_3 network by the cotton candy-templating method. In brief, the cotton candy was firstly fabricated through centrifugal spinning via cotton-candy-machine; then, the continuous cotton candy fibers were dissolved in the water, leaving hollow channels inside the polymer matrix; the hollow channels were replaced by the fillers via vacuum-assisted impregnation and high-pressure treatment (Fig. 3a). The fabricated Al_2O_3/epoxy composites had a continuous filler network (Fig. 3b) and a 15-fold enhancement in TC at 36.2 vol% compared with pristine epoxy (Fig. 3c).

Ice-templated method Ice-templated method is also a novel method to construct the filler network, and it always combines with infiltrating method to prepare polymer composites. For example, Chen et al. [71] constructed the cellulose nanofiber-supported 3D interconnected BNNS (3D-C-BNNS) aerogels via sol–gel and freeze-drying method based on self-assembled BNNSs on a 3D cellulose skeleton (Fig. 4a). The epoxy matrix was introduced into the space among filler network by infiltration. The epoxy composites exhibited a continuous filler network (Fig. 4b), and an ultrahigh TC of 3.13 W/(mK) was achieved at a low BNNS content of 9.6 vol% (Fig. 4c). Besides, the TC could be easily enhanced by tailoring the BNNS loading in the interconnected 3D network.

The ice-templated method is always employed to orient the filler for an enhanced TC in the special direction
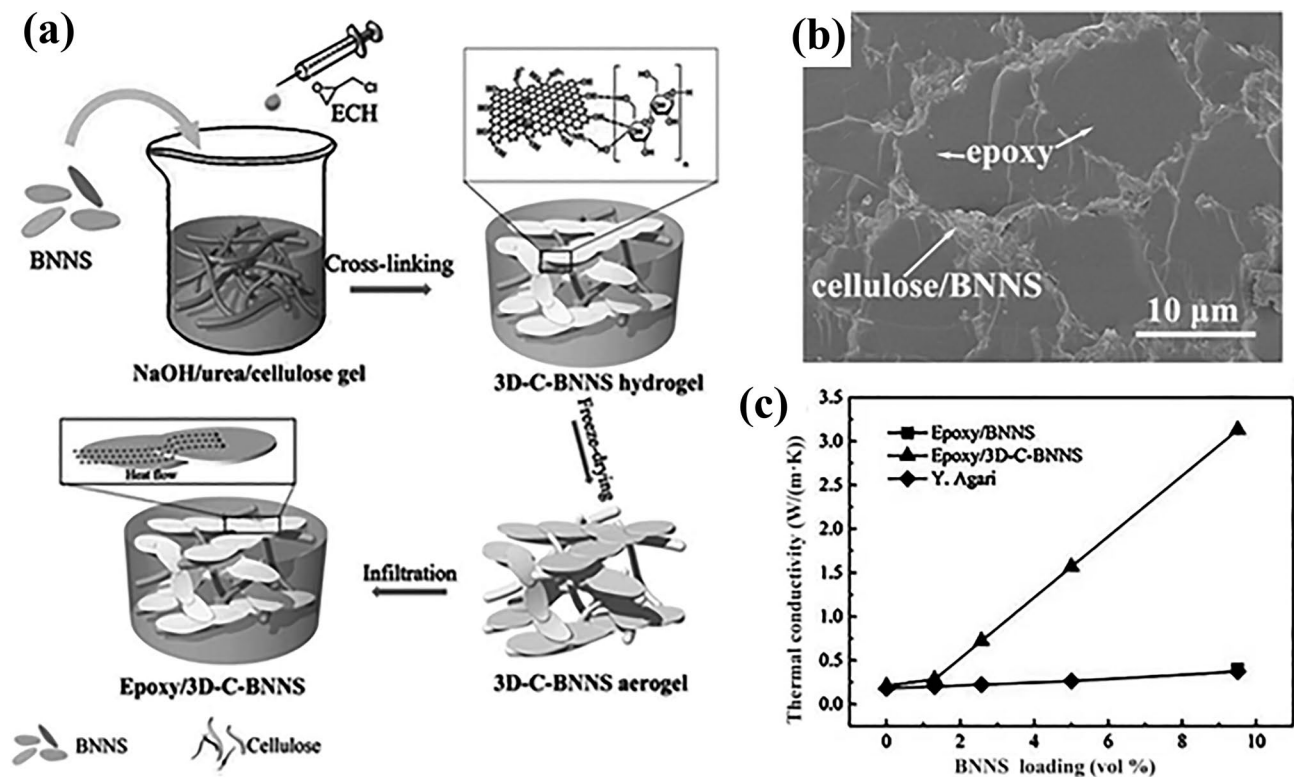
Fig. 4 (**a**) Preparation of epoxy composites. (**b**) The cross-sectional SEM image of epoxy composites with 9.6 vol% BNNS. (**c**) TCs of epoxy composites as a function of filler content. [71] (Images reprinted with permission from [66].)

of polymer composites. So far, fillers of CNTs, BN [72–76], and SiC [77] have been oriented well by the ice-templating method. For example, Zeng et al. [75] studied the ice-templating approach to successfully construct the oriented 3D BN nanosheets (3D-BNNS) network (Fig. 5a). The obtained polymer composites exhibited an oriented 3D-BNNS aerogel path for phonons (Fig. 5b). The TC of products reached 2.85 W/mK at a relatively low BNNS content of 9.29 vol% (Fig. 5c). Later, Yao et al. [74] introduced the reduced graphene oxide (r-Go) into the above 3D-BNNS network. An ultrahigh through-plane TC of 5.05 W/(mK) was obtained. Hu et al. [73] combined the ice-templating method and infiltration method to fabricate the ordered 3D-BN networks. It was found that the TCPC possessed a TC up to 4.42 W/mK at a filler content of 34 vol%, much higher than that of the counterpart with random 3D-BN (1.81 W/mK) and counterpart with random BN (1.16 W/(mK)).

Generally, in a word, these artificially controlled methods are efficient to construct the filler networks, but they normally need multiple processes and they are often time consuming, so it is difficult for mass fabrication.

2.4.2 Double continuous network

A double continuous networking system typically contains fillers and two immiscible polymers. With appropriate fractions of two immiscible polymers and appropriate temperature and enthalpy, a double continuous structure with selected location of fillers in one polymer could be obtained, and the one containing fillers acts as continual conductive network [78]. Each double continuous structure has its best volume ratio [79–82]. For instance, the two immiscible polymers of PBT and PC were mixed together with GNPs, and a continual conductive network of PBT/GNPs was constructed well when the volume ratio of PBT to PC was 50:50 [79], as illustrated in Fig. 6.

Generally, the location of fillers in immiscible polymer matrices commonly lies on the interfacial energies between components and the viscosity of polymers. In theory, once the thermodynamic equilibrium was achieved, the localization of fillers was determined by the interfacial energy. The thermodynamic equilibrium for the localization of fillers can be estimated from wetting coefficient (w_a) based on Young's equation [80].
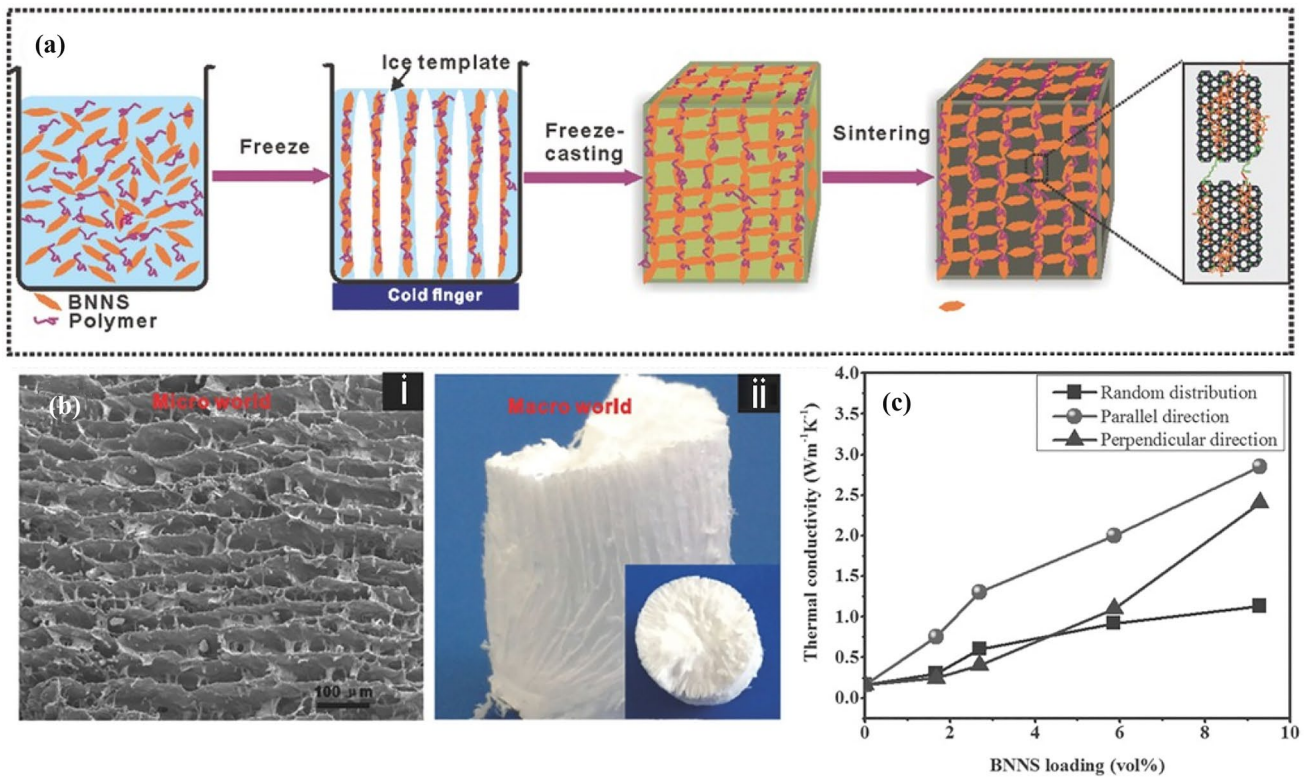
Fig. 5 (**a**) Diagram of the prepared 3D-BNNS aerogels. (**b**) Hierarchical structures of the free-standing 3D-BNNS aerogel: (i) SEM image of 3D-BNNS aerogel in the perpendicular direction to ice growth; (ii) photograph of a 3D-BNNS aerogel. (**c**) TCs of products as a function of BNNS content. (Images reprinted with permission from [70].)

$$w_a = \frac{\gamma_{f-PA} - \gamma_{f-PB}}{\gamma_{PA-PB}} \tag{1}$$

where γ is the interfacial energy between components. When $w_a < -1$, the filler is preferentially located in phase A; when $-1 < w_a < 1$, the filler is located at the interface between phases A and B; when $w_a > 1$, the filler is preferentially located in phase B.

The interfacial energy γ was calculated by the harmonic mean Eq. (2) and geometric mean Eq. (3) [83].

Fig. 6 Schematic diagram of PBT/PC/GNP composites with various volume ratio of PBT to PC: (**a**) 70/30, (**b**) 50/50, and (**c**) 30/70 [79]. (Images reprinted with permission from [74].)
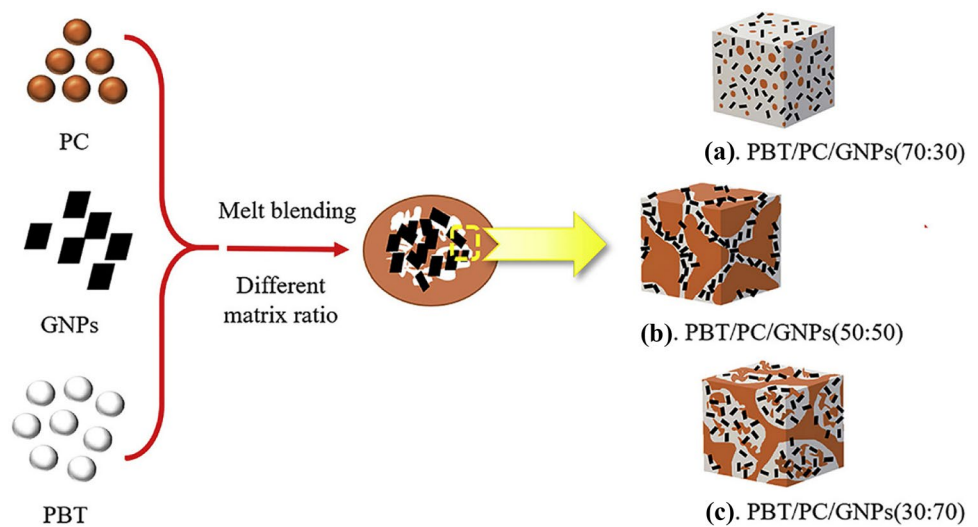
Table 1 TCs of polymer composites with double continuous network

No	Polymer A/B/fillers	TCs of polymer composites with double continuous network-filler content W/(mK)	TCs of polymer composites with self-assembled network-filler-content W/(mK)	TCs of fillers W/(mK)
1	HDPE/PMMA/CNF [86]	0.65–16 wt%	0.54 (HDPE/CNF)–16 wt%	Axial 1400 [87]
2	PBT/PC/GNP [79]	0.352–3 vol%	0.38 (PBT/GNPs)–3 vol%	100–400 [88]
3	PP/EPDM/BN [89]	1.37–40 wt%	0.9 (PP/BN)–40 wt%	185–300 [88]
4	PP/PS/BN [90]	5.57–50 wt%	2.02 (PS/BN)–50 wt%	
5	SEBS/PP/BN [91]	1.3–3 phr	0.42 (SEBS/PP)	
6	LDPE/PS/CNT [92]	0.275–1.5 wt%	0.18 (PS/LDPE)	1000–4000 [88]
7	PC/PA66/AlN/CNT [93]	1.3–24.78 vol%	0.2 (PC/PA66)	
8	PVDF/PS/SiC/CNT [94]	1.85–24.78 vol%	0.14 (PVDF/PS)	
9	PCL/PBS/PC/CNT [95]	0.44–4 wt%	0.15 (PCL/PBS)	
10	PA6/PP/graphite [96]	4.722–50 wt%	~4.3 (PA6/graphite)	100–400 [88]

LTEG low-temperature expandable graphite, *GNP* graphite nanoplatelet, *CNF* carbon nanofiber

$$\gamma_{1-2} = \gamma_1 + \gamma_2 - 4\left[\frac{\gamma_1^d \gamma_2^d}{\gamma_1^d + \gamma_2^d} + \frac{\gamma_1^p \gamma_2^p}{\gamma_1^p + \gamma_2^p}\right] \quad (2)$$

$$\gamma_{1-2} = \gamma_1 + \gamma_2 - 2\left[\sqrt{(\gamma_1^d \gamma_2^d)} + \sqrt{(\gamma_1^p \gamma_2^p)}\right] \quad (3)$$

where γ^d and γ^p are the disperse component and polar component of the surface energy of the component, respectively.

Over the past decades, it has already been proved that the double continuous networking method is effective to enhance the electrical conductivity and low down the percolation threshold of electrical conductivity [84, 85]. In these years, this method is becoming popular to enhance the TCs of TCPCs with two immiscible polymers, such as HDPE/PMMA, PBT/PC, PP/PS, LDPE/PS, and PC/PA66, as shown in Table 1.

Obviously, the results (in Table 1) show that the double continuous networking method plays an important role in the greater enhancement of TCs, compared with the traditional self-assembled network at the same or a lower filler content. The double continuous network can also be constructed by selecting polymers with different melt temperatures. For example, Zhou et al. [97] prepared a double continuous network in Elvaloy and PBT matrices based on the different melting temperature between Elvaloy and PBT. A TC up to 7.8 W/(mK) was obtained as LTED was introduced into Elvaloy/PBT matrices. Briefly, the LTEG and Elvaloy were firstly mixed by an internal mixer at a temperature of 170 ℃. After that, the PBT was introduced into Elvaloy-LTEG mixtures and mixed together by the internal mixer at a temperature of 170 ℃. Finally, the samples for different measurements were fabricated with thickness of approximately

4 mm using a hot pressing method at 10 MPa and 240 °C to keep the network architecture intact (Fig. 7).

2.4.3 Segregated filler network

In order to maximize the utilization efficiency of the fillers, forming the segregated structures in the TCPCs has becoming a promising method, where the fillers are selectively located at the interfaces of polymer particles by drying or solution mixing.

In the last decade, numbers of researchers have devoted to the design and develop the segregated 3D architectures. For example, Hu et al. [98] reported a 3D-segregated network of AlN in the PP matrix to improve the TCs of TCPCs (Fig. 8a). The AlN was selectively located at the PP particles by the mechanical grinding method, and a TC of 0.81 W/(mK) was obtained at 30 vol% AlN. A segregated structure of graphite constructed in UHMPE matrix by the binder-mixing method and solvent-mixing method (Fig. 8b), respectively, was reported by Feng et al. [99]. The TCs of UHMPE composites were improved to 2.276 and 1.883 W/(mK) with the graphite content of 18.83 vol%, respectively. Jiang et al. [100] reported a TC of 4.15 W/(mK) for a segregated filler network of BN in PPS matrix by chemical cross-linking (Fig. 8c). The TC of 2.45 W/(mK) exhibited 1.69 times higher than PPS/BN composite at the same BN content. Ding et al. [101] reported a 3D-segregated network of BN in the PI matrix by a hot pressing method. Herein, the BN was firstly coated on the surface of PI granules via the PI adhesive to form a core–shell structure; after that, the BN-PI granules were transformed to the segregated network by hot embossing. The TC of BN/PI composites reached up to 4.47 W/(mK) at 20 vol%.
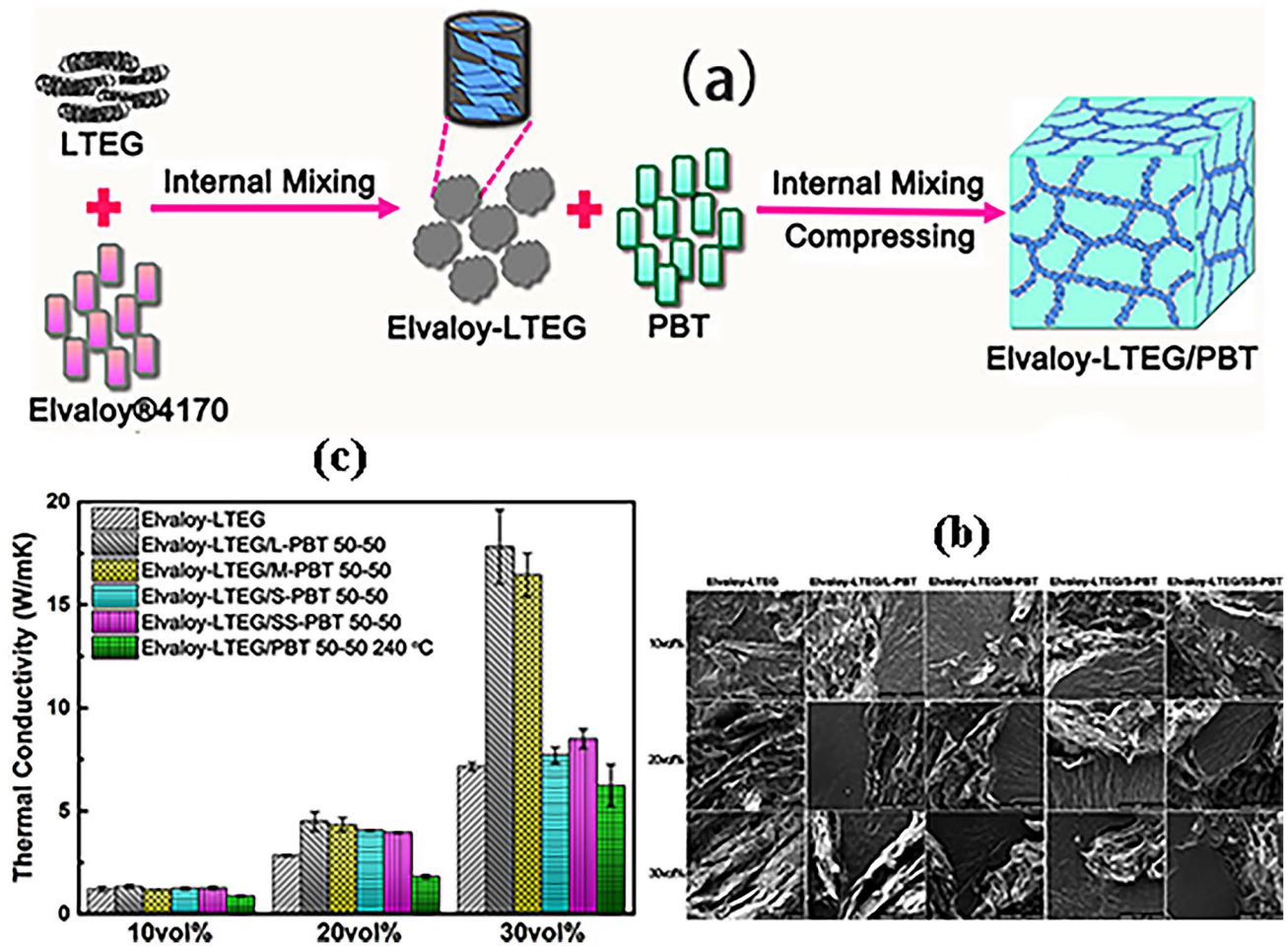
Fig. 7 (**a**) Fabrication process of Elvaloy-LTEG/PBT composites with the segregated network. (**b**) SEM pictures of segregated network in Elvaloy-LTEG/PBT composites. (**c**) TC of Elvaloy-LTEG/PBT composites as a function of LTEG content and PBT particles size [97]. (Images reprinted with permission from [92].)

Segregated structures with hybrid filler system were also reported. A TC of 7.1 W/(m/K) in UHMWPE composite with hybrid segregated structure of AlN/BN was reported by Wang et al. [102]. Herein, AlN and BN were firstly mechanically wrapped upon UHMWPE granules, and after that they were consolidated with high-pressure to form segregated structure. Wu et al. [103] reported a TC of 1.08 W/(mK) in polystyrene composites with a unique hybrid segregated filler network of GNPs/MWCNT (3.5/1.5 wt%). A segregated structure with a hybrid filler system was further studied to balance the TC and electrical insulation performance for thermal management applications. Zhang et al. [104] reported a TC up to 2.69 W/(m K) in PA 6 composites with a hybrid segregated filler network of graphene nanoplatelets (GNPs)/BN, almost tenfold improvement in TC of pure PA6, and an electrical conductivity as low as $4.13 \times 10-9$ S/m. Wang et al. [105] constructed a segregated filler network with hybrid filler of BN and CNT. The

PVDF composites exhibited a TC of up to 1.8 W/(mK), much higher than PVDF composites with BN/CNT random structure or segregated BN structure.

2.4.4 Hybrid fillers

A combination of two or more fillers mixed as hybrid fillers can generate synergistic effects to enhance the TC, which is superior to that achievable with any TCPCs consisting of either filler alone. The synergistic effects always occur when each filler is dissimilar to the other in size and aspect ratio. In one aspect, smaller fillers locating between larger fillers can provide a path between the two larger fillers in which heat may flow between the larger fillers with no or less distance traversed through the highly insulating matrix. In another aspect, fillers with a higher aspect ratio can efficiently connect fillers with smaller aspect ratio even when the content of the former

Fig. 8 Mechanism of segregated filler network by (**a**) mechanical grinding [98], (**b**) solution method [99], and (**c**) chemical cross-linking [100]. (Images reprinted with permission from [93–95].)
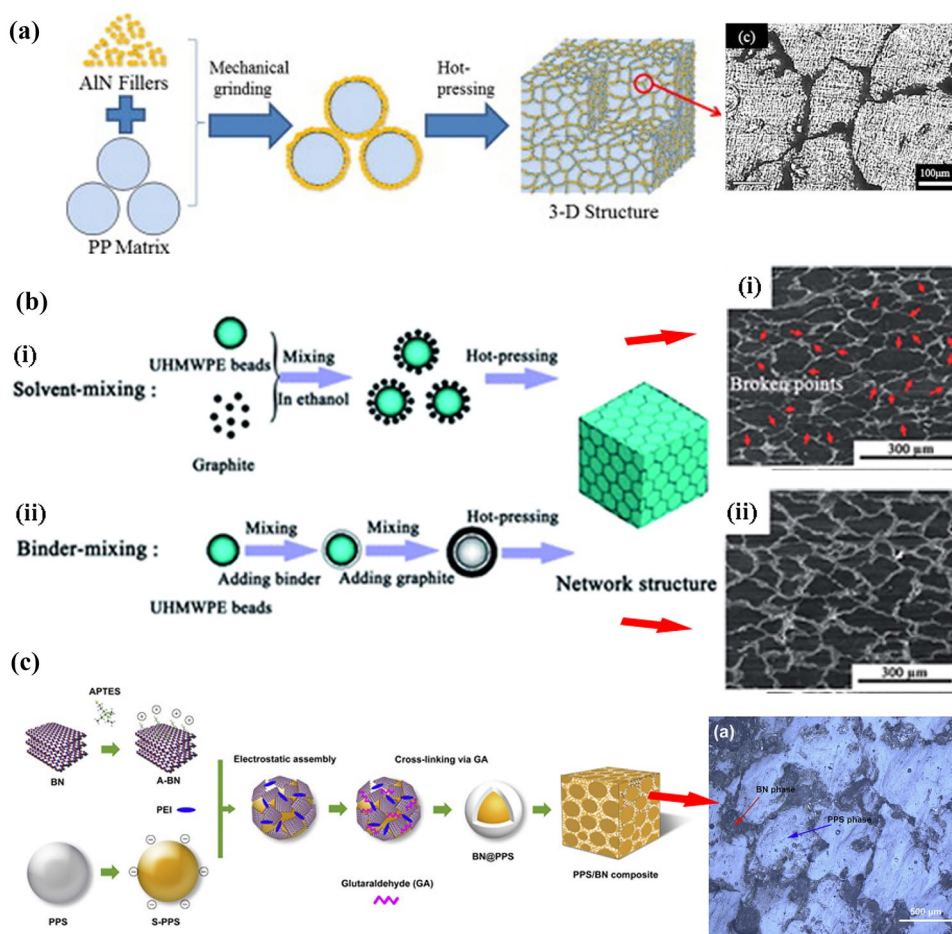
is relatively low. Figure 9 illustrates the common hybrid fillers designed with different aspect ratios and sizes in the TCPCs.

A hybrid filler system consisting of quasi-1D fibers and spherical fillers is shown in Fig. 9a. CFs, CNTs, and AlN whiskers, as the typical quasi-1D fillers, were always

Fig. 9 Illustration of different strategies for the used hybrid fillers in TCPCs. Hybrid fillers of (**a**) quasi-1D fibers and spherical fillers, (**b**) quasi-1D fibers with different size, (**c**) spherical fillers with different radii, (**d**) quasi-2D fillers and quasi-1D, (**e**) quasi-2D fillers and spherical particles, and (**f**) quasi-2D fillers with different material or size
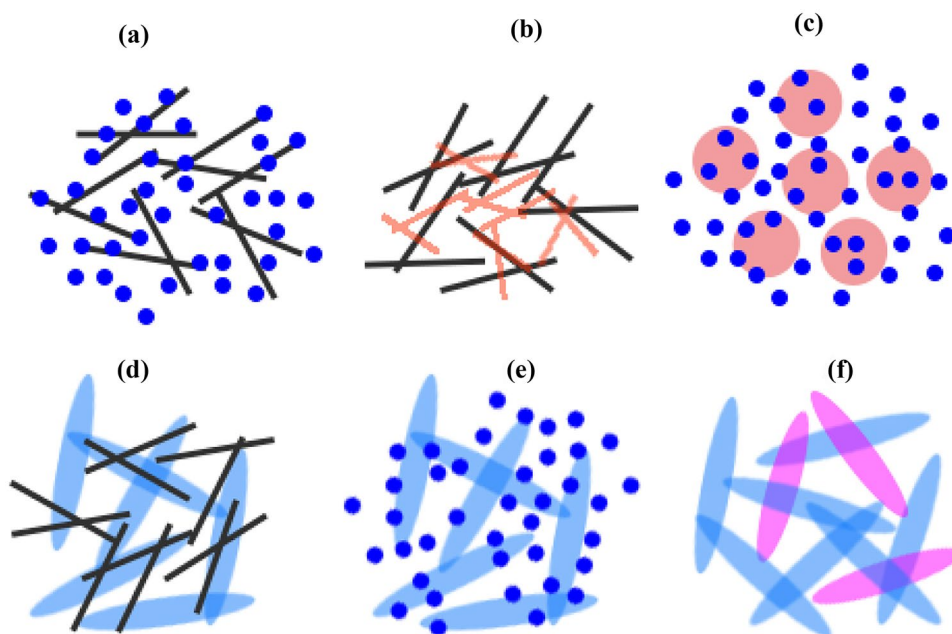
combined with spherical fillers of Al_2O_3 [106, 107], spherical AlN [93, 108], and SiO_2 [109]. For example, Dang et al. [110] investigated PVDF composites filled with anisotropic AlN whiskers and isotropic spheres AlN. A maximum TC of 4.321 W/(mK) at 60 vol% (volume ratios of former to latter is 1:1) was achieved because the AlN spheres successfully served as wedges between AlN whiskers to promote the construction of the 3D filler network. Oh et al. [109] studied TC of epoxy composites filled with CNT and spherical SiO_2. A maximum TC value of 0.340 W/(mK) at 0.6 wt% CNT and SiO_2 was achieved, higher than composites only with SiO_2.

The hybrid filler system that consisted of quasi-1D fillers with different sizes is shown in Fig. 9b. CNTs and CFs were always combined together, as the CNTs can serve as wedges between CFs to promote the formation of filler network [27, 111–117]. The hybrid filler of CNTs and CFs could also induce a three-dimensional hierarchical network for the enhanced TC in and through thickness of samples even though the TCs of CNT and CF are anisotropic. Ji and co-workers [111] employed the chemical vapor deposition (CVD) method and electrostatic flocking device to align the CNT and CF respectively in and through thickness of silastic composites. The TCs up to 7.51 and 3.72 W/mK through and in-plane of samples were achieved.

A hybrid filler system that consisted of spherical fillers with different radii is shown in Fig. 9c. So far, the hybrid spherical filler systems of Al_2O_3/AlN [118] and Al_2O_3/SiC [119] have already been reported. It was concluded that the hybrid spherical filler systems were important in the high TC of TCPCS because as the spherical fillers with different sizes were mixed, small particle fillers easily entered the gap between large particle fillers, so the porosity between fillers was easily reduced and the packing density was easily increased, and more heat chains were formed for the heat flow.

Figure 9d shows a hybrid filler system that consisted of quasi-2D fillers and quasi-1D particles. Herein, graphene, graphite, and BN, as the typical quasi-2D particles, have attracted growing attention in recent years to build a hybrid filler system because the adjacent quasi-2D fillers can be easily bridged by the quasi-1D fillers, which simultaneously strengthens the interfacial connection and forms a highly conducting network for heat flow. So far, the hybrid filler systems of BN/CNT [105, 120–125], BN/CF [126–128], graphene/CuNWs [129], BN/SiC [130], graphene/SiC [45], and graphene/CNTs [131–133], have already been reported in the literature. The results all indicated that the presence of synergistic effect in hybrid polymer composites contributed to the high TC, not the utilization of single fillers.

Figure 9e shows a hybrid filler system consisted of quasi-2D fillers and spherical fillers. Synergetic

enhancement of TC was reported in this hybrid filler system because hybrid fillers can create more pathways for phonon transport. The hybrid filler systems of BN/spherical AlN [134, 135], graphene/AlN [136], graphene/Al_2O_3 [137–139], BN/Al_2O_3 [140–143], BN/SiO_2 [144], and BN/AgNPs [145] were widely reported. In addition, since the quasi-2D fillers afford strong anisotropic TC, TCPCs generally exhibit high in-plane TC while low through-plane TC. In order to improve the through-plane TC, spherical fillers were introduced to disrupt the alignment of quasi-2D fillers along the lateral direction during processing. For example, Pan et al. [146] used the h-BN platelets and AlN particles as hybrid fillers to improve the through-plane TC of PTFE. It was concluded that AlN particles effectively disrupt the alignment of h-BN platelets along the lateral direction during the compression processing and a high through-plane TC up to 1.04 W/mK was achieved at 30 vol% filler content, 3.8 times that of neat PTFE.

Quasi-2D filler and quasi-2D fillers with different sizes or materials were often investigated as a hybrid filler system, as shown in Fig. 9f. BN, graphene, and graphite nanoplate were always used to form a hybrid filler system to improve the TC [104, 147–149]. Zhang et al. [104] fabricated a core–shell structures by GNPs and BN to form a continuous filler network. A TC up to 2.69 W/(mK) in nylon 6 composites was achieved, almost tenfold improvement in TC of pure PA6. Due to the conductive network of GNPs cut off by the BN segregated layer, an electrical conductivity as low as $4.13 \times 10 - 9$ S/m was obtained. Lewis et al. [148] also presented similar results in the epoxy composites with hybrid fillers of graphene and BN fillers (21.8 vol% in total). Herein, the hybrid fillers of graphene and BN were intentionally chosen with similar thickness, lateral dimensions, and aspect ratios. A TC up to 6.5 W/(mK) was obtained in epoxy composites. Xing et al. [150] introduced hybrid fillers of graphite nanoplates with small size around 1–5 μm and large size around 20 μm into the epoxy matrix. A TC of 1.33 W/(mK) was achieved at 20 wt% (weight ratios of large particles to small particles is 17:3).

2.4.5 Filler orientation

Many thermally conductive fillers have anisotropic TC. These fillers always have a non-spherical shape, such as quasi-2D fillers (BN, graphene, graphite flakes) and quasi-1D fillers (CF, CNT). These fillers can be oriented during processing to achieve a high TC in the direction of orientation, but a low TC perpendicular to the direction of orientation. Shear or stretching forces, external fields, ice-templating, 3D printing, and CVD are the methods often used to orient the fillers, as shown in Fig. 10.

Shear or stretching forces can make the fillers arrange along the shear or stretching direction to form a conductive
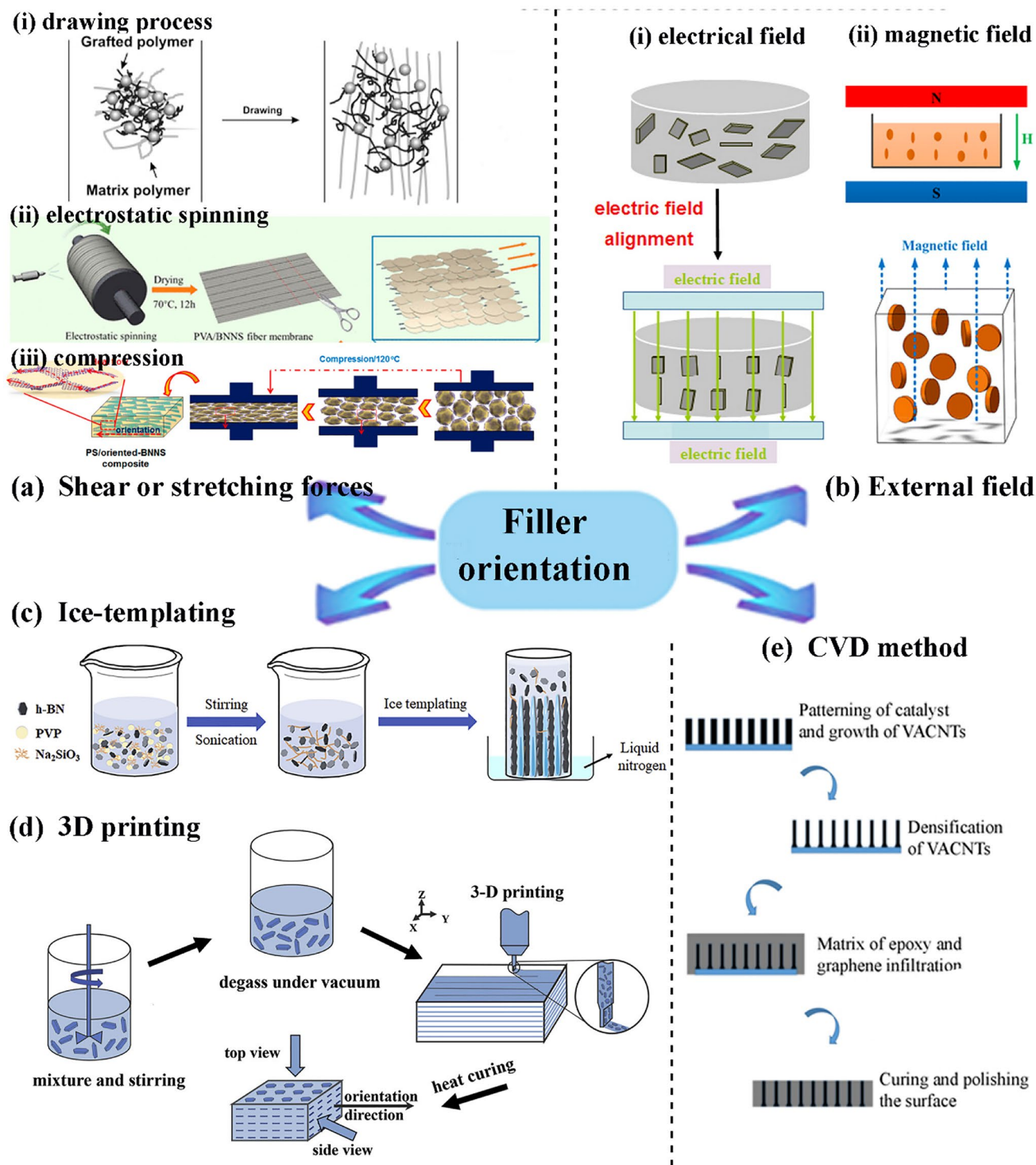
Fig. 10 Illustration of methods to orient fillers in the polymer. (**a**) Shear or stretching forces, e.g., (i) drawing process [151], (ii) electrostatic spinning [152], and (iii) compression [153]. (**b**) External fields, e.g., (i) electrical field [154] and (ii) magnetic field [155]. (**c**) Ice-templating [72]. (**d**) 3D printing [140]. (**e**) Chemical vapor deposition (CVD) [156]. (Images reprinted with permission from [67, 134, 145–150].)

path. Shear or stretching forces are from processing of drawing process [151], electrostatic spinning [152, 157, 158], compression [19, 153, 159–164], 3D printing [140, 165],

milling [41, 166–168], injection [169–171], and casting [172]. Some processes are shown in Fig. 10a.

The magnetic field is often utilized to orient the fillers (Fig. 10b). The magnetic substances, such as Fe_3O_4 and FeCo, are often coated on the surface of fillers for the magnetic property of fillers. Yuan et al. [155] used the magnetic field to orient the BN platelets coated with superparamagnetic iron oxide nanoparticles. The TC of TCPCs with oriented BN, parallel to the heat flux direction, was 44.5% higher than that of composites with unaligned BN at filler content of 9.14 vol%. Shi et al. [44] used the external magnetic field to align multilayer graphene (MG) modified by Fe_3O_4 in the silicon rubber (SR) matrix. The Fe_3O_4@ MG/SR composites possessed a high TC of 0.64 W/(mK) in the alignment direction. Yan et al. [173] used the magnetic field to align graphene nanosheets (GNSs) coated with Fe_3O_4. The epoxy composites possessed a high TC in the direction of heat flow at low Fe_3O_4@GNS loadings, much higher than the composites with randomly dispersed bare GNSs. Kim et al. [174] used the magnetic field to orient the BN in the polymer matrix. An enhancement of 1.96-fold (at filler content of 30 vol%) in TC was obtained for the synthesized vertically aligned composites. Other scholars [175–177] have also studied the external magnetic field to orient the BN to improve the TC in the direction of heat flow.

The electric field with alternating current (AC) or directing current (DC) voltage has already been applied to orient the fillers, as shown in Fig. 10b. The substances, such as TiO_2, are often coated on the surface of fillers to enhance the dielectric property. Guo et al. [154] induced the graphene orientation in PVDF via DC electrical field. A TC up to 0.587 W/(mK) at 20 wt% was achieved, 4.5% higher than that before aligning graphene. The coated BN with TiO_2 used to prepare TiO_2@BN/polyurethane acrylate composite via external electric field with 500–700 kHZ and 600 V AC voltage was reported by Kim et al. [178]. The TC reached to 1.54 W/(mK), 1.9-fold (at filler content of 20 vol%) higher than the counterpart with randomly oriented BN (0.78 W/(mK)). Liu et al. [179] introduced an AC electrical field to align the clay nanoparticles along the thickness direction in the PDMS matrix. The obtained TC up to 0.316 W/(mK) in through-plane of composites was around 1.6 times higher than the counterpart with nonaligned clay nanoparticles at 5 wt%.

Recently, the ice-templated method was widely used to orient fillers, as shown in Fig. 10c, and many examples have been introduced in part 2.4.1. Other methods of 3D printing and CVD have also been used to prepare the oriented filler network (Fig. 10d, e). For example, Shao et al. [156] induced the vertically aligned CNT arrays (VACNT) by the CVD method in the epoxy matrix. The longitudinal TC of 1.85 W/(mK) was obtained due to the contracted vertical heat transfer channels in the film, as shown in Fig. 10e.

3 Conclusions and outlook

The continuous filler network plays a significant role to enhance the thermal conductivity of polymer composite. The formation of the filler network is a function of filler aspect ratio, content, and size. It is a must for us to take a holistic approach when designing the filler network. In this review, we mainly discussed these main affecting factors of the filler network. The preparing methods also greatly affect the formation of the network. Herein, the methods of 3D self-assembled networking, double continuous networking, segregated filler networking, hybrid fillers, and filler orientation, to deal with the filler network, have been summarized.

Although some successes of polymer composites have already been obtained by scholars, there are still many challenges for thermally conductive polymer composites. More studies are expected in the following aspects. First, most reported methods to construct the continuous filler network are time consuming, costly, and relatively complicated. Thus, they still needed further studies for simple and mass production. Other novel and simple methods also need to be further explored to prepare polymer composites. Second, a significant amount of fillers is often required to achieve a high thermal conductivity in polymer composite. However, the high filler loading often fails to achieve the expected high thermal conductivity, and often results in the deterioration of mechanical and processing properties, as well as a high cost. So, further studies should be conducted to balance the above properties of polymer composites. Finally, even though a great enhancement in thermal conductivity was reported in some literature, the thermal conductivity of polymer composites was still much less than the instinct thermal conductivity of filler; thus, the mechanism of this phenomena needs to be further studied, excluding the theory of the thermally conductive path theory, the thermal percolation theory, and the thermoelastic coefficient.

Declarations

Conflict of Interest The authors declare no competing interests.

References

1. Huang Y et al (2019) Tailoring the electrical and thermal conductivity of multi-component and multi-phase polymer composites. Int Mater Rev 65(3):129–163

2. Pradhan SS et al (2020) Thermally conducting polymer composites with EMI shielding: a review. J Electron Mater 49(3):1749–1764

3. Guo Y et al (2020) Factors affecting thermal conductivities of the polymers and polymer composites: a review. Compos Sci Technol 193:108134

4. Kashfipour MA, Mehra N, Zhu J (2018) A review on the role of interface in mechanical thermal and electrical properties of polymer composites. Adv Compos Hybrid Mater 1(3):415–439

5. Yu W et al (2018) Advanced thermal interface materials for thermal management. Eng Sci 2(9):1–3

6. Guo Y et al (2018) Significantly enhanced and precisely modeled thermal conductivity in polyimide nanocomposites with chemically modified graphene via in situ polymerization and electrospinning-hot press technology. J Mater Chem C 6(12):3004–3015

7. Zhang P et al (2017) Thermal properties of graphene filled polymer composite thermal interface materials. Macromol Mater Eng 302(9):1700068

8. Altay L et al (2019) Synergistic effects of graphene nanoplatelets in thermally conductive synthetic graphite filled polypropylene composite. Polym Compos 40(1):277–287

9. Yang X et al (2018) A review on thermally conductive polymeric composites: classification measurement model and equations mechanism and fabrication methods. Adv Compos Hybrid Mater 1(2):207–230

10. Xu Z et al (2020) Enhanced thermal conductivity and electrically insulating of polymer composites. J Mater Sci 56(6):4225–4238

11. Pan C et al (2017) Improved thermal conductivity and dielectric properties of hBN/PTFE composites via surface treatment by silane coupling agent. Compos Part B Eng 111:83–90

12. Deng S et al (2016) Effect of chain structure on the thermal conductivity of expanded graphite/polymer composites. RSC Adv 6(12):10185–10191

13. Wei B, Zhang L, Yang S (2021) Polymer composites with expanded graphite network with superior thermal conductivity and electromagnetic interference shielding performance. Chem Eng J 404:126437

14. Sun J et al (2021) The contribution of conductive network conversion in thermal conductivity enhancement of polymer composite: a theoretical and experimental study. ES Mater Manuf 13:53–65

15. Yang Y et al (2017) Effect of microstructure on thermal conductivity of polymer composites. Macromol Res 25(4):344–351

16. Yuan H et al (2019) Fabrication of thermal conductive and electrically insulating polymer composites with isotropic thermal conductivity by constructing a three-dimensional interconnected network. Nanoscale 11(23):11360–11368

17. Ouyang Y et al (2020) Design of network Al_2O_3 spheres for significantly enhanced thermal conductivity of polymer composites. Compos Part A Appl Sci Manuf 128:105673

18. Li M et al (2020) Highly thermal conductive and electrical insulating polymer composites with boron nitride. Compos Part B Eng 184:107746

19. Yu C et al (2018) Hot-pressing induced alignment of boron nitride in polyurethane for composite films with thermal conductivity over 50Wm/K. Compos Sci Technol 160:199–207

20. Hong H et al (2019) Anisotropic thermal conductive composite by the guided assembly of boron nitride nanosheets for flexible and stretchable electronics. Adv Funct Mater 37(37):1902575

21. Krause B, Rzeczkowski P, Pötschke P (2019) Thermal conductivity and electrical resistivity of melt-mixed polypropylene composites containing mixtures of carbon-based fillers. Polymer 11(6):1073

22. Xie P et al (2021) Hierarchically porous Co/C nanocomposites for ultralight high-performance microwave absorption. Adv Compos Hybrid Mater 4(1):173–185

23. Wang M et al (2020) Graphdiyne for significant thermal conductivity enhancement at ultralow mass fraction in polymer composites. 2D Mater 7(3):035007

24. Shtein M et al (2015) Thermally conductive graphene-polymer composites: size percolation and synergy effects. Chem Mater 27(6):2100–2106

25. Chen J et al (2020) Recent progress on thermo-electrical properties of conductive polymer composites and their application in temperature sensors. Eng Sci 12(14):13–22

26. Nidamanuri N et al (2020) Graphene and graphene oxide-based membranes for gas separation. Eng Sci 9(7):3–16

27. He X et al (2019) Enhancing thermal conductivity of polydimethylsiloxane composites through spatially confined network of hybrid fillers. Compos Sci Technol 172:163–171

28. Zhou S et al (2020) Preparation of thermally conductive polycarbonate/boron nitride composites with balanced mechanical properties. Polym Compos 41(12):5418–5427. https://doi.org/10.1002/pc.25805

29. Kim K et al (2014) Chemically modified boron nitride-epoxy terminated dimethylsiloxane composite for improving the thermal conductivity. Ceram Int 40(1):2047–2056

30. Shen M et al (2011) Thermal conductivity model of filled polymer composites. Int J Miner Metall Mater 18(5):623–631

31. Patti A et al (2016) The effect of filler functionalization on dispersion and thermal conductivity of polypropylene multi wall carbon nanotubes composites. Compos Part B Eng 94:350–359

32. Song J et al (2019) Thermal conductivity of natural rubber nanocomposites with hybrid fillers. Chin J Chem Eng 27(4):928–934

33. Zhang DL et al (2018) Enhanced thermal conductivity and mechanical property through boron nitride hot string in polyvinylidene fluoride fibers by electrospinning. Compos Sci Technol 156:1–7

34. Guiney LM et al (2018) Three-dimensional printing of cytocompatible thermally conductive hexagonal boron nitride nanocomposites. Nano Lett 18(6):3488–3493

35. Yang B et al (2020) Filler network structure in graphene nanoplatelet (GNP)-filled polymethyl methacrylate (PMMA) composites: from thermorheology to electrically and thermally conductive properties. Polym Test 89:106575

36. Lee J et al (2019) Optimizing filler network formation in poly(hexahydrotriazine) for realizing high thermal conductivity and low oxygen permeation. Polymer 179:121639

37. Fan X, Yin X (2018) Progress in research and development on matrix modification of continuous fiber-reinforced silicon carbide matrix composites. Adv Compos Hybrid Mater 1(4):685–695

38. Das TK, Ghosh P, Das NC (2019) Preparation development outcomes and application versatility of carbon fiber-based polymer composites: a review. Adv Compos Hybrid Mater 2(2):214–233

39. Du B et al (2021) Multifunctional carbon nanofiber-SiC nanowire aerogel films with superior microwave absorbing performance. Adv Compos Hybrid Mater 1–11

40. Kim CY et al (2019) The alignment of AlN platelets in polymer matrix and its anisotropic thermal properties. J Materiomics 5(4):679–687

41. Wang H et al (2019) Highly anisotropic thermally conductive polyimide composites via the alignment of boron nitride platelets. Compos Part B Engineering 158:311–318

42. Geng Y et al (2019) Enhanced through-plane thermal conductivity of polyamide 6 composites with vertical alignment of boron nitride achieved by fused deposition modeling. Polym Compos 40(2):3375–3382

43. Han J et al (2019) An anisotropically high thermal conductive boron nitride/epoxy composite based on nacre-mimetic 3D network. Adv Funct Mater 29(13):1900412

44. Shi Y et al (2019) Magnetically aligning multilayer graphene to enhance thermal conductivity of silicone rubber composites. J Appl Polym Sci 136(37):47951

45. Song J, Zhang Y (2020) Vertically aligned silicon carbide nanowires/reduced graphene oxide networks for enhancing the thermal conductivity of silicone rubber composites. Compos Part A Appl Sci Manuf 133:105873

46. Bustero I et al (2020) Free-standing graphene films embedded in epoxy resin with enhanced thermal properties. Adv Compos Hybrid Mater 3(1):31–40

47. George J, Ishida H (2018) A review on the very high nanofiller-content nanocomposites: Their preparation methods and properties with high aspect ratio fillers. Prog Polym Sci 86:1–39

48. Stunda-Zujeva A, Irbe Z, Berzina-Cimdina L (2017) Controlling the morphology of ceramic and composite powders obtained via spray drying – a review. Ceram Int 43(15):11543–11551

49. Su CY et al (2014) Cosmetic properties of TiO_2/mica-BN composite powder prepared by spray drying. Ceram Int 40(5):6903–6911

50. Barick P et al (2016) Spray-freeze-dried nanosized silicon carbide containing granules: properties compaction behaviour and sintering. J Eur Ceram Soc 36(16):3863–3877

51. Su KH et al (2019) Development of thermally conductive polyurethane composite by low filler loading of spherical BN/PMMA composite powder. Sci Rep 9(1):14397

52. Ren L et al (2019) Spray-assisted assembled spherical boron nitride as fillers for polymers with enhanced thermally conductivity. Chem Eng J 370:166–175

53. Shin YK et al (2013) Effect of BN filler on thermal properties of HDPE matrix composites. Ceram Int 39:569–573

54. Tarhini A et al (2021) The effect of graphene flake size on the properties of graphene-based polymer composite films. J Appl Polym Sci 138(6):49821

55. Moradi S et al (2019) Achieving high thermal conductivity in epoxy composites: effect of boron nitride particle size and matrix-filler interface. Polymer 11(7):1156

56. Jasmee S et al (2021) Interface thermal resistance and thermal conductivity of polymer composites at different types shapes and sizes of fillers: a review. Polym Compos 42(6):2629–2652

57. Han MS et al (2009) Electrical morphological and rheological properties of carbon nanotube composites with polyethylene and poly(phenylenesulfide) by melt mixing. Chem Eng Sci 64(22):4649–4656

58. Song YS, Youn JR (2005) Influence of dispersion states of carbon nanotubes on physical properties of epoxy nanocomposites. Carbon 43(7):1378–1385

59. Zhou WY et al (2007) Study on insulating thermal conductive BN/HDPE composites. Thermochim Acta 452(1):36–42

60. Zhang S et al (2011) The effects of particle size and content on the thermal conductivity and mechanical properties of Al_2O_3/high density polyethylene (HDPE) composites. Express Polym Lett 5(7):581–590

61. Wu D et al (2017) Spatial confining forced network assembly for preparation of high-performance conductive polymeric composites. Compos Part A Appl Sci Manuf 102:88–95

62. Wang J et al (2018) Enhancing dielectric performance of poly(vinylidene fluoride) nanocomposites via controlled distribution of carbon nanotubes and barium titanate nanoparticles. Eng Sci 4(24):79–86

63. Fang C et al (2020) Calculating the electrical conductivity of graphene nanoplatelet polymer composites by a monte carlo method. Nanomaterials 10(6):1129

64. Gkourmpis T et al (2019) Melt-mixed 3D hierarchical graphene/polypropylene nanocomposites with low electrical percolation threshold. Nanomaterials 9(12):1766

65. Du F et al (2006) An infiltration method for preparing single-wall nanotube/epoxy composites with improved thermal conductivity. J Polym Sci Part B Polym Phys 44(10):1513–1519

66. Xiao C et al (2019) Three dimensional porous alumina network for polymer composites with enhanced thermal conductivity. Compos Part A Appl Sci Manuf 124:105511

67. Yin L et al (2016) Fabrication of a polymer composite with high thermal conductivity based on sintered silicon nitride foam. Compos Part A Appl Sci Manuf 90:626–632

68. Liu Z et al (2016) Exceptionally high thermal and electrical conductivity of three-dimensional graphene-foam-based polymer composites. RSC Adv 6(27):22364–22369

69. Liu Z et al (2019) Graphene foam embedded epoxy composites with significant thermal conductivity enhancement. Nanoscale 11(38):17600–17606

70. Wu Y et al (2019) Cotton candy-templated fabrication of three-dimensional ceramic pathway within polymer composite for enhanced thermal conductivity. ACS Appl Mater Interfaces 11(47):44700–44707

71. Chen J et al (2017) Cellulose nanofiber supported 3D interconnected BN nanosheets for epoxy nanocomposites with ultrahigh thermal management capability. Adv Funct Mater 27(5):1604754

72. Wu F et al (2020) Thermal conductivity of polycaprolactone/three-dimensional hexagonal boron nitride composites and multi-orientation model investigation. Compos Sci Technol 197:108245

73. Hu J et al (2017) Polymer composite with improved thermal conductivity by constructing a hierarchically ordered three-dimensional interconnected network of BN. ACS Appl Mater Interfaces 9(15):13544–13553

74. Yao Y et al (2018) Construction of 3D skeleton for polymer composites achieving a high thermal conductivity. Small 14(13):e1704044

75. Zeng X et al (2015) Ice-templated assembly strategy to construct 3D boron nitride nanosheet networks in polymer composites for thermal conductivity improvement. Small 11(46):6205–6213

76. Wang X, Wu P (2019) 3D vertically aligned BNNS network with long-range continuous channels for achieving a highly thermally conductive composite. ACS Appl Mater Interfaces 11(32):28943–28952

77. Yao Y et al (2018) Vertically aligned and interconnected SiC nanowire networks leading to significantly enhanced thermal conductivity of polymer composites. ACS Appl Mater Interfaces 10(11):9669–9678

78. Lin S et al (2019) Key factors in mechanical reinforcement by double percolation network: Particle migration and shear stability of filler network. Polymer 182:121820

79. Wen B, Zheng X (2019) Effect of the selective distribution of graphite nanoplatelets on the electrical and thermal conductivities of a polybutylene terephthalate/polycarbonate blend. Compos Sci Technol 174:68–75

80. Amoabeng D et al (2020) Fumed silica induces co-continuity across a wide composition range in immiscible polymer blends. Polymer 186:121831

81. Sultana SMN et al (2019) Tailoring MWCNT dispersion blend morphology and EMI shielding properties by sequential mixing strategy in immiscible PS/PVDF blends. J Electron Mater 49(3):1588–1600

82. Roman C et al (2020) Effect of selective distribution of MWCNTs on the solid-state rheological and dielectric properties of blends of PMMA and LDPE. J Mater Sci 55(20):8526–8540

83. Zhang Z et al (2019) Improvement of the thermal/electrical conductivity of PA6/PVDF blends via selective MWCNTs-NH_2 distribution at the interface. Mater Des 177:107835

84. Lan Y et al (2016) Electrically conductive thermoplastic polyurethane/polypropylene nanocomposites with selectively distributed graphene. Polymer 97:11–19

85. Huang J et al (2014) Control of carbon nanotubes at the interface of a co-continuous immiscible polymer blend to fabricate conductive composites with ultralow percolation thresholds. Carbon 73:267–274

86. Kashfipour MA et al (2019) Carbon nanofiber reinforced co-continuous HDPE/PMMA composites: Exploring the role of viscosity ratio on filler distribution and electrical/thermal properties. Compos Sci Technol 184:107859

87. Beechem et al (2016) Thermal conductivity of turbostratic carbon nanofiber networks. J Heat Transfer 138(6):1–9

88. Chen H et al (2016) Thermal conductivity of polymer-based composites: Fundamentals and applications. Prog Polym Sci 59:41–85

89. Cao M et al (2019) Effect of the blending processes on selective localization and thermal conductivity of BN in PP/EPDM Co-continuous blends. Polym Test 78:105978

90. Liu B et al (2020) Highly thermally conductive polystyrene/polypropylene/boron nitride composites with 3D segregated filler networks prepared by solution-mixing and hot-pressing method. Chem Eng J 385(1):123829

91. Zhang D et al (2017) High thermal conductivity and excellent electrical insulation performance in double-percolated three-phase polymer nanocomposites. Compos Sci Technol 144:36–42

92. Kwon Y (2014) Anisotropic thermal conductive MWCNT/polymer composites prepared with an immiscible PS/LDPE blend. J Nanosci Nanotechnol 14(8):6146–6149

93. Xiao C et al (2018) Improved thermal properties by controlling selective distribution of AlN and MWCNT in immiscible polycarbonate (PC)/Polyamide 66 (PA66) composites. Compos Part A Appl Sci Manuf 110:133–141

94. Cao J et al (2013) High thermal conductivity and high electrical resistivity of poly(vinylidene fluoride)/polystyrene blends by controlling the localization of hybrid fillers. Compos Sci Technol 89:142–148

95. Gumede TP et al (2019) Isothermal crystallization kinetics and morphology of double crystalline PCL/PBS blends mixed with a polycarbonate/MWCNTs masterbatch. Polymer 11(4):682

96. Zhou S et al (2015) Enhanced thermal conductivity of polyamide 6/polypropylene (PA6/PP) immiscible blends with high loadings of graphite. J Compos Mater 50(3):327–337

97. Zhou H et al (2017) Significant enhancement of thermal conductivity in polymer composite via constructing macroscopic segregated filler networks. ACS Appl Mater Interfaces 9(34):29071–29081

98. Hu M, Feng J, Ng KM (2011) Thermally conductive PP/AlN composites with a 3-D segregated structure. Compos Sci Technol 110:26–34

99. Feng CP et al (2016) Highly thermally conductive UHMWPE/graphite composites with segregated structures. RSC Adv 6(70):65709–65713

100. Jiang Y et al (2017) BN@PPS core-shell structure particles and their 3D segregated architecture composites with high thermal conductivities. Compos Sci Technol 144:63–69

101. Ding D et al (2019) Highly thermally conductive polyimide composites via constructing 3D networks. Macromol Rapid Commun 40(17):1800805

102. Wang ZG et al (2018) Synergetic enhancement of thermal conductivity by constructing hybrid conductive network in the segregated polymer composites. Compos Sci Technol 162(7):7–13

103. Wu K et al (2017) Design and preparation of a unique segregated double network with excellent thermal conductive property. ACS Appl Mater Interfaces 9(8):7637–7647

104. Zhang X et al (2019) Preparation of highly thermally conductive but electrically insulating composites by constructing a segregated double network in polymer composites. Compos Sci Technol 175:135–142

105. Wang ZG et al (2018) Enhanced thermal conductivity of segregated poly(vinylidene fluoride) composites via forming hybrid conductive network of boron nitride and carbon nttttanotubes. Ind Eng Chem Res 57(31):10391–10397

106. Wang H et al (2020) Efficient thermal transport highway construction within epoxy matrix via hybrid carbon fibers and alumina particles. ACS Omega 5(2):1170–1177

107. Li H et al (2019) Enhanced thermal conductivity by combined fillers in polymer composites. Thermochim Acta 676:198–204

108. Zhang X et al (2018) Thermal conductivity of rubber composite materials with a hybrid AlN/carbon fiber filler. Chin Sci Bull 63(23):2403–2410

109. Oh Y et al (2019) Investigation of mechanical thermal and electrical properties of hybrid composites reinforced with multi-walled carbon nanotubes and fused silica particles. Carbon Lett 30(4):353–365

110. Dang TML et al (2017) Enhanced thermal conductivity of polymer composites via hybrid fillers of anisotropic aluminum nitride whiskers and isotropic spheres. Compos Part B Eng 114:237–246

111. Ji T et al (2018) Thermal conductive and flexible silastic composite based on a hierarchical framework of aligned carbon fibers-carbon nanotubes. Carbon 131:149–159

112. Yang J et al (2016) Three-dimensional-linked carbon fiber-carbon nanotube hybrid structure for enhancing thermal conductivity of silicon carbonitride matrix composites. Carbon 108:38–46

113. Singh AK et al (2017) Aligned multi-walled carbon nanotubes (MWCNT) and vapor grown carbon fibers (VGCF) reinforced epoxy adhesive for thermal conductivity applications. J Mater Sci Mater Electron 28(23):17655–17674

114. Tülbez S, Esen Z, Dericioglu AF (2020) Effect of CNT impregnation on the mechanical and thermal properties of C/C-SiC composites. Adv Compos Hybrid Mater 3(2):177–186

115. Han D et al (2019) Macroscopic carbon nanotube assembly/silicon carbide matrix composites produced by gas phase route. Adv Compos Hybrid Mater 2(1):142–150

116. He Y et al (2021) Reinforce the mechanical toughness heat resistance and friction and wear resistance of phenolic resin via constructing self-assembled hybrid particles of graphite oxide and zirconia as nano-fillers. Adv Compos Hybrid Mater 4(2):317–323

117. Zhang D et al (2020) Overview of ultrasonic assisted manufacturing multifunctional carbon nanotube nanopaper based polymer nanocomposites. Eng Sci 10(14):35–50

118. Li D et al (2019) Effect of different size complex fillers on thermal conductivity of PA6 thermal composites. Plast Rubber Compos 48(8):347–355

119. Vaisakh SS et al (2016) Effect of nano-modified SiO_2/Al_2O_3 mixed-matrix micro-composite fillers on thermal mechanical and tribological properties of epoxy polymers. Polym Adv Technol 27(7):905–914

120. Ji B et al (2020) Mussel inspired interfacial modification of boron nitride/carbon nanotubes hybrid fillers for epoxy composites with improved thermal conductivity and electrical insulation properties. J Polym Res 27(8):1–12

121. An D et al (2019) Flexible thermal interfacial materials with covalent bond connections for improving high thermal conductivity. Chem Eng J 383:123151

122. Wang Y et al (2020) Achieving a 3D thermally conductive while electrically insulating network in polybenzoxazine with a novel hybrid filler composed of boron nitride and carbon nanotubes. Polymer 12(10):2331

123. Xiao YJ et al (2016) Largely enhanced thermal conductivity and high dielectric constant of poly(vinylidene fluoride)/boron nitride composites achieved by adding a few carbon nanotubes. J Phys Chem C 120(12):6344–6355

124. Guo Y et al (2019) Largely enhanced thermal conductivity and thermal stability of ultra high molecular weight polyethylene composites via BN/CNT synergy. RSC Adv 9(70):40800–40809

125. Su Z et al (2018) Fabrication of thermal conductivity enhanced polymer composites by constructing and oriented three-dimensional staggered interconnected network of boron nitride platelets and carbon nanotubes. ACS Appl Mater Interfaces 10(42):36342–36351

126. Cheewawuttipong W et al (2014) Thermal conductivity of polypropylene composites with hybrid fillers of boron nitride and vapor-grown carbon fiber. Polym Compos 37(3):1–8

127. Owais M et al (2019) Synergetic effect of hybrid fillers of boron nitride graphene nanoplatelets and short carbon fibers for enhanced thermal conductivity and electrical resistivity of epoxy nanocomposites. Compos Part A Appl Sci Manuf 117:11–22

128. Jiang X et al (2020) Simultaneously enhancing the thermal conductivity and dielectric constant of BN/CF hybrid filled polypropylene/polystyrene composites via in situ reactive processing. Polym Compos 41(4):1234–1241

129. Li M et al (2018) A thermally conductive and insulating epoxy polymer composite with hybrid filler of modified copper nanowires and graphene oxide. J Mater Sci 29(6):4948–4954

130. Wang B et al (2020) Highly thermally conductive PVDF-based ternary dielectric composites via engineering hybrid filler networks. Compos Part B Eng 191:107978

131. Duan G et al (2019) Preparation of PMIA dielectric nanocomposite with enhanced thermal conductivity by filling with functionalized graphene–carbon nanotube hybrid fillers. Appl Nanosci 9(8):1743–1757

132. Li Q et al (2020) Enhanced thermal conductivity and isotropy of polymer composites by fabricating 3D network structure from carbon-based materials. J Appl Polym Sci 138(5):49781

133. Zhou Y et al (2018) High-performance thermal management nanocomposites: silver functionalized graphene nanosheets and multiwalled carbon nanotube. Curr Comput-Aided Drug Des 8(11):398

134. Liang D et al (2020) Synergetic enhancement of thermal conductivity by constructing BN and AlN hybrid network in epoxy matrix. J Polym Res 27(8):1–12

135. Cho JK et al (2020) Heat dissipative mechanical damping properties of EPDM rubber composites including hybrid fillers of aluminium nitride and boron nitride. Soft Matter 16(29):6812–6818

136. Yuan W et al (2016) Thermal conductivity of epoxy adhesive enhanced by hybrid graphene oxide/AlN particles. Appl Therm Eng 106:1067–1074

137. Akhtar MW et al (2017) Alumina-graphene hybrid filled epoxy composite: quantitative validation and enhanced thermal conductivity. Compos Part B Eng 131:184–195

138. Yu W et al (2016) Synergistic improvement of thermal transport properties for thermoplastic composites containing mixed alumina and graphene fillers. J Appl Polym Sci 133(13):43242

139. Huang H et al (2020) Morphological mechanical and thermal properties of PA6 nanocomposites Co-Incorporated with Nano-Al$_2$O$_3$ and graphene oxide fillers. Polymer 188:122119

140. Liu M et al (2020) Polymer composites with enhanced thermal conductivity via oriented boron nitride and alumina hybrid fillers assisted by 3-D printing. Ceram Int 46(13):20810–20818. https://doi.org/10.1016/j.ceramint.2020.05.096

141. Song H et al (2019) Synergistic effects of various ceramic fillers on thermally conductive polyimide composite films and their model predictions. Polymer 11(3):484

142. Mai VD et al (2019) Rheological properties and thermal conductivity of epoxy resins filled with a mixture of alumina and boron nitride. Polymer 11(4):597

143. Yan H et al (2021) Flexible thermally conductive and electrically insulating silicone rubber composite films with BNNS@Al$_2$O$_3$ fillers. Adv Compos Hybrid Mater 4(1):36–50

144. Gao C, Shen Y, Wang T (2020) Enhanced thermal conductivity for traditional epoxy packaging composites by constructing hybrid conductive network. Mater Res Express 7(6):p065308

145. Wu Y et al (2020) Synergistic effects of boron nitride (BN) nanosheets and silver (Ag) nanoparticles on thermal conductivity and electrical properties of epoxy nanocomposites. Polymer 12(2):426

146. Pan C et al (2018) Enhanced through-plane thermal conductivity of PTFE composites with hybrid fillers of hexagonal boron nitride platelets and aluminum nitride particles. Compos Part B Eng 153:1–8

147. Yang J et al (2018) Hybrid network structure of boron nitride and graphene oxide in shape-stabilized composite phase change materials with enhanced thermal conductivity and light-to-electric energy conversion capability. Sol Energ Mater Sol Cell 174:56–64

148. Lewis JS et al (2019) Thermal and electrical conductivity control in hybrid composites with graphene and boron nitride fillers. Mater Res Express 6(8):085325

149. An D et al (2019) A polymer-based thermal management material with enhanced thermal conductivity by introducing three-dimensional networks and covalent bond connections. Carbon 155:258–267

150. Xing Z et al (2019) Size-controlled graphite nanoplatelets: thermal conductivity enhancers for epoxy resin. J Mater Sci 54(13):10041–10054

151. Ruan WH et al (2007) Effects of processing conditions on properties of nano-SiO$_2$/polypropylene composites fabricated by pre-drawing technique. Compos Sci Technol 67(13):2747–2756

152. Chen J et al (2017) Vertically aligned and interconnected boron nitride nanosheets for advanced flexible nanocomposite thermal interface materials. ACS Appl Mater Interface 9(36):30909–30917

153. Wang X, Wu P (2017) Preparation of highly thermally conductive polymer composite at low filler content via a self-assembly process between polystyrene microspheres and boron nitride nanosheets. ACS Appl Mater Interfaces 9(23):19934–19944

154. Guo H et al (2016) Thermal conductivity of graphene/poly(vinylidene fluoride) nanocomposite membrane. Mater Des 114(15):355–363

155. Yuan C et al (2015) Thermal conductivity of polymer-based composites with magnetic aligned hexagonal boron nitride platelets. ACS Appl Mater Interface 7(23):13000–13006

156. Shan B et al (2019) Preparation of graphene/aligned carbon nanotube array composite films for thermal packaging applications. Jpn J Appl Phys 58(SH):SHHH01

157. Ziyadi H et al (2021) An investigation of factors affecting the electrospinning of poly (vinyl alcohol)/kefiran composite nanofibers. Adv Compos Hybrid Mater 1–12

158. Yang S et al (2018) Thermal and mechanical performance of electrospun chitosan/poly(vinyl alcohol) nanofibers with graphene oxide. Adv Compos Hybrid Mater 1(4):722–730

159. Tan SC et al (2016) Compression-induced graphite nanoplatelets orientation in fibre-reinforced plastic composites. Compos Part B Eng 90:493–502

160. Park HJ, Woo JS, Park SY (2019) Poly (phenylene sulfide)-graphite composites for bipolar plates with preferred morphological orientation. Korean J Chem Eng 36(12):2133–2142

161. Park HJ, Woo JS, Park SY (2019) Poly(phenylene sulfide)-graphite composites for bipolar plates with preferred morphological orientation. Korean J Chem Eng 36(12):2133–2142

162. Yu C et al (2018) Hot pressing-induced alignment of hexagonal boron nitride in SEBS elastomer for superior thermally conductive composites. RSC Adv 8(45):25835–25845

163. Ohayon-Lavi A et al (2020) Compression-enhanced thermal conductivity of carbon loaded polymer composites. Carbon 163:333–340

164. Sun J et al (2019) Development and application of hot embossing in polymer processing: a review. ES Mater Manuf 6(4):3–17

165. Mei H et al (2019) Tailoring strength and modulus by 3D printing different continuous fibers and filled structures into composites. Adv Compos Hybrid Mater 2(2):312–319

166. Feng CP et al (2018) A facile route to fabricate highly anisotropic thermally conductive elastomeric POE/NG composites for thermal management. Adv Mater Interface 5(2):1700946

167. Ou X et al (2020) Enhancement of thermal conductivity and dimensional stability of polyimide/boron nitride films through mechanochemistry. Compos Commun 23:100549

168. Feng CP et al (2017) Electrically insulating POE/BN elastomeric composites with high through-plane thermal conductivity fabricated by two-roll milling and hot compression. Adv Compos Hybrid Mater 1(1):160–167

169. Ren Y et al (2019) A trade-off study toward highly thermally conductive and mechanically robust thermoplastic composites by injection moulding. Compos Sci Technol 183:107787

170. Rudresh BM, Ravi Kumar BN, Madhu D (2019) Combined effect of micro- and nano-fillers on mechanical thermal and morphological behavior of glass–carbon PA66/PTFE hybrid nano-composites. Adv Compos Hybrid Mater 2(1):176–188

171. Fu H et al (2020) Overview of injection molding technology for processing polymers and their composites. ES Mater Manuf 8:3–23

172. Lule ZC, Oh H, Kim J (2020) Enhanced directional thermal conductivity of polylactic acid/polybutylene adipate terephthalate ternary composite filled with oriented and surface treated boron nitride. Polym Test 86:106495

173. Yan H et al (2015) Thermal conductivity of magnetically aligned graphene–polymer composites with Fe_3O_4-decorated graphene nanosheets. J Electron Mater 44(2):658–666

174. Kim K, Kim J (2016) Vertical filler alignment of boron nitride/epoxy composite for thermal conductivity enhancement via external magnetic field. Int J Therm Sci 100:29–36

175. Yuan J et al (2019) Highly thermally conducting polymer-based films with magnetic field-assisted vertically aligned hexagonal boron nitride for flexible electronic encapsulation. ACS Appl Mater Interface 11(19):17915–17924

176. Su Z et al (2018) Fabrication of thermal conductivity enhanced polymer composites by constructing an oriented three-dimensional staggered interconnected network of boron nitride platelets and carbon nanotubes. ACS Appl Mater Interface 10(42):36342–36351

177. Yuan F et al (2017) Surface modification and magnetic alignment of hexagonal boron nitride nanosheets for highly thermally conductive composites. RSC Adv 7(69):43380–43389

178. Kim K, Ju H, Kim J (2016) Filler orientation of boron nitride composite via external electric field for thermal conductivity enhancement. Ceram Int 42(7):8657–8663

179. Liu Z et al (2018) Electric-field-induced out-of-plane alignment of clay in poly(dimethylsiloxane) with enhanced anisotropic thermal conductivity and mechanical properties. Compos Sci Technol 165:39–47

Dr. Xiaoxiang He is a lecturer in Xiangtan University. She got her Ph.D. degree from Beijing University of Chemical Technology. Her research interests focus on polymer processing, polymer composites, and polymer-based functional devices.

Dan Ou is a graduate student candidate now in Xiangtan University. Her research interests focus on polymer processing and polymer composites.

Dr. Prof. Shuying Wu is an associate professor in Xiangtan University. Her research interests focus on the phase change materials and heat and mass transfer.

Dr. Yue Luo got his Ph.D. degree from South China University of Technology. His research interests focus on phase change materials, polymer processing and polymer composites.

Dr. Ying Ma is a lecturer in Xiangtan University. Her research interests focus on phase change materials and heat and mass transfer.

Dr. Prof. Jingyao Sun got his Ph.D. degree from Beijing University of Chemical Technology and is now doing research in Beijing University of Chemical Technology as an associate professor. His research interests focus on polymer composites, polymer processing, and polymer-based functional devices, including flexible sensors, thermal interface materials, soft robotics, and so on.